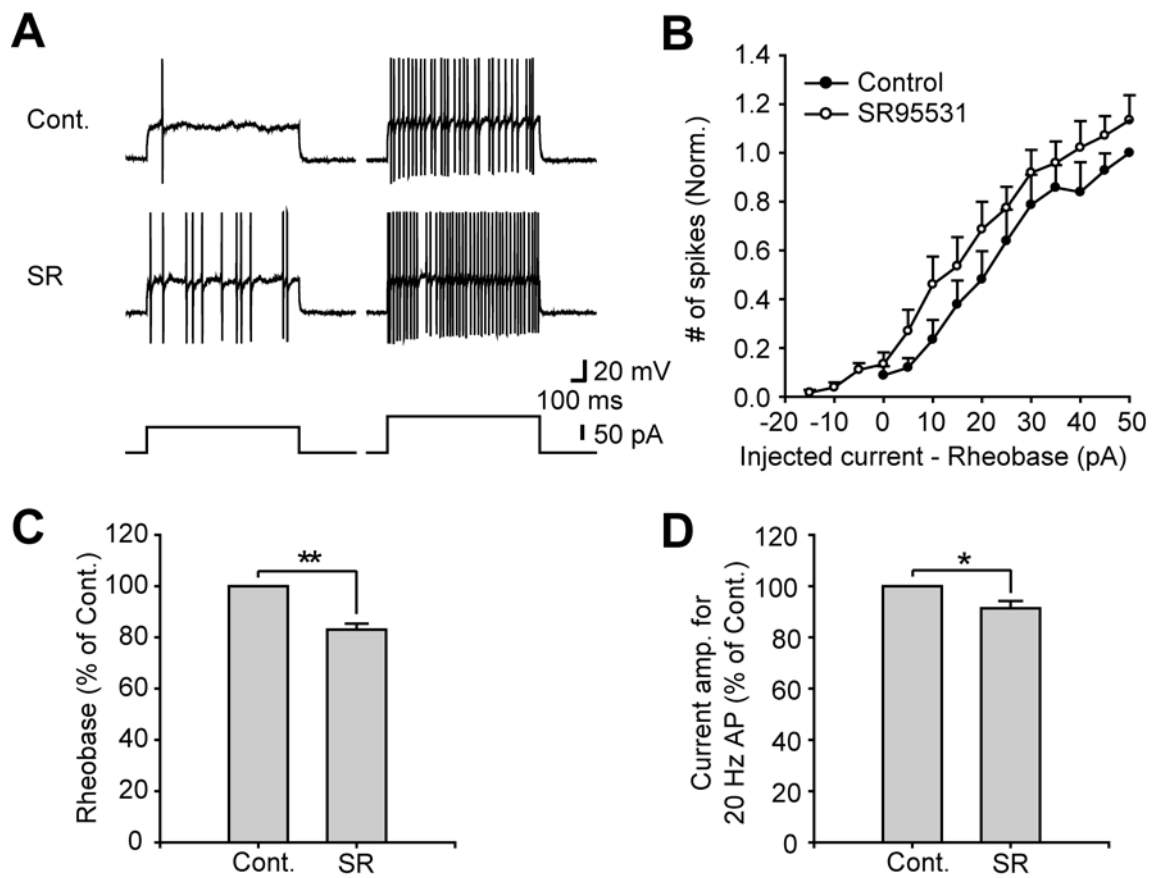


Supplemental Figure 1

Four distinct firing patterns in dorsal horn EGFP+ neurons. (A-D) Top; Responses to depolarizing current steps. Middle; Injected current. Bottom, Output firing frequency and input current (F-I) relationship in neurons corresponding to top panels. Closed circles indicate the number of action potentials while open circles indicate the mean instantaneous frequency ($\langle F \rangle$) in the current injection protocol (1 sec, 0 to 120 or 240 pA increment of 5 or 10 pA). (A) Tonic-firing neurons were characterized by linearly increased response over a wide range of stimulation intensities. (B) Delayed-firing neurons showed a delay (arrow) between the onset of the current pulse and the first action potential even after higher current injections. (C) Phasic-

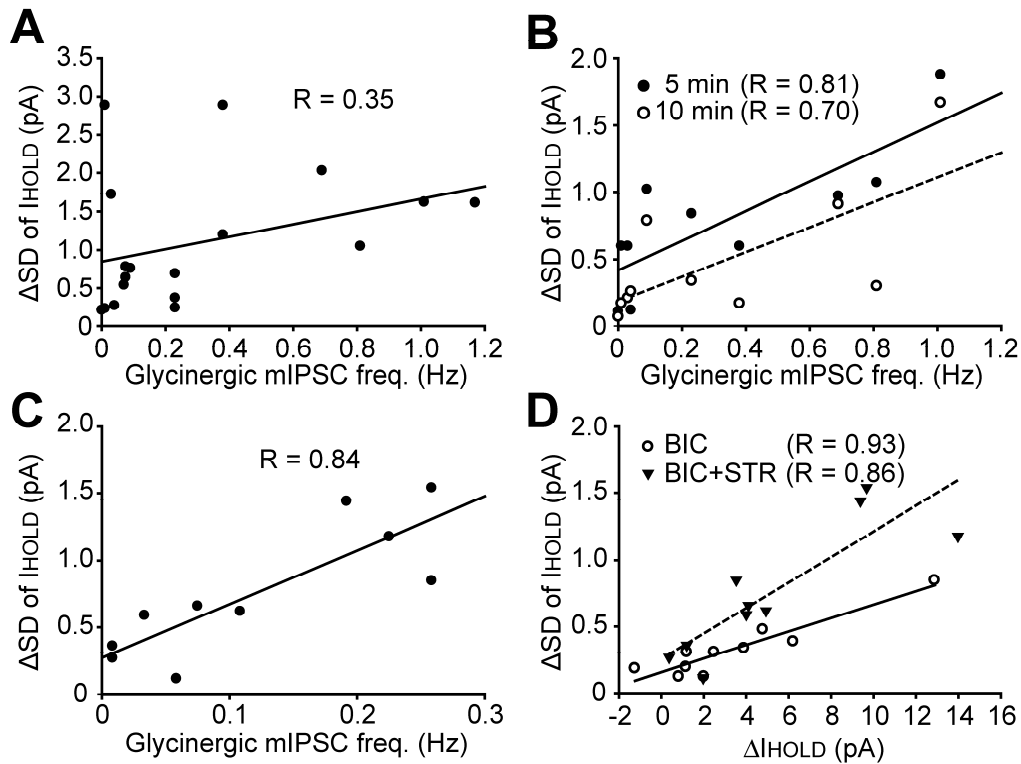
firing neurons tended not to respond to mild stimulation with repetitive firing and instead showed an abrupt increase in frequency as the stimulus intensity was increased above rheobase.

(D) Single-spike neurons generated only one or a few action potentials at the beginning of the current pulse at just suprathreshold pulses.



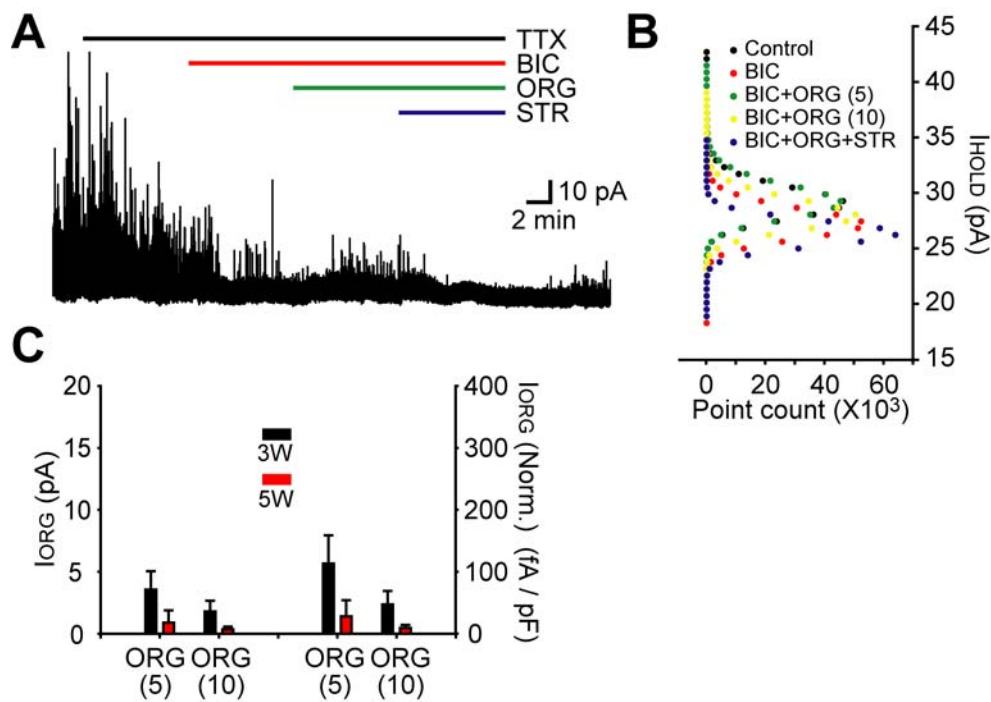
Supplemental Figure 2

The effect of SR95531 on EGFP+ cell excitability. (A) Typical examples of action potentials induced by current injection (85 pA; left, 120 pA; right panel) under 2 conditions (Control; NBQX (10 μ M) and AP5 (50 μ M), SR; NBQX, AP5 and SR95531 (30 μ M)). Resting membrane potential was kept at -65 mV. Bottom traces show injected currents. (B) F-I relationship of EGFP+ neurons before and after application of SR (n = 6). (C) SR decreased the rheobase (n = 6). (D) SR decreased the current amplitude required for action potential firing at 20 Hz (n = 6). Data are shown as means \pm SEM. * P < 0.05, ** P < 0.01.



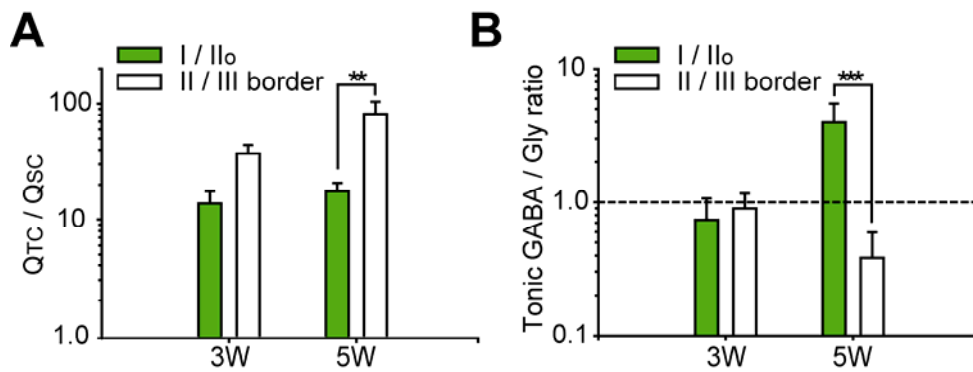
Supplemental Figure 3

Standard deviation of holding current (SD of I_{HOLD}) changed with pharmacological manipulation. (A) The change in SD of I_{HOLD} after application of strychnine was not correlated with the glycinergic mIPSC frequency at 3W ($n = 18$). (B) The changes in SD of I_{HOLD} 5 and 10 min after application of ORG were correlated with the glycinergic mIPSC frequency ($n = 10$, 5 min; filled circles and black line, 10 min, open circles and dotted line). (C) The change in SD of I_{HOLD} after application of strychnine was correlated with the glycinergic mIPSC frequency at 5W ($n = 10$). (D) The decrease in I_{HOLD} and in SD of I_{HOLD} under BIC and BIC+STR conditions was correlated at 5W ($n = 10$, BIC; open circles and black line, BIC+STR; filled triangles and dotted line).



Supplemental Figure 4

Effect of glycine transporter 1 inhibitor, ORG 24598, in GABA d EGFP+ neurons obtained from 5W animals. (A) Baseline shift is shown as induced by bicuculline, followed by co-application with ORG 24598 (ORG; 10 μM) and finally ORG plus strychnine. Holding membrane potentials was 0 mV. (B) All-points histograms plot the amplitude of I_{HOLD} under different conditions (control; black circles, after application of bicuculline (BIC); red circles, 5 and 10 min after co-application of ORG (BIC+ORG (5) and (10)); green and yellow circles, after co-application of strychnine (BIC+ORG+STR); blue circles). (C) There was no difference in I_{ORG} (left columns) or I_{ORG} normalized by cell capacitance (right columns) between the neurons obtained from 3W ($n = 6$) and 5W ($n = 4$) animals. The scale was kept with the same as Figure 5G to facilitate comparison. Data are shown as means \pm SEM.



Supplemental Figure 5

Synaptic and tonic charge transfer through glycine and GABA_A receptors. (A) The ratio for inhibitory charge carried by total tonic and synaptic conductance (Q_{TC} / Q_{SC}) was greater in Lamina II/III border neurons (3W; n = 9, 5W; n = 6, white bars) than in lamina I/Ilo neurons (3W; n = 9, 5W; n = 4, green bars) at 5W but not at 3W. (B) The ratios for negative charge transfer through tonic GABA_AR- and GlyR-mediated conductance (tonic GABA/Gly ratio) in lamina I/Ilo and in lamina II/III border neurons were not different at 3W, but were different at 5W. Data are shown as means \pm SEM. ** P < 0.01, *** P < 0.001, two-way ANOVA with post hoc Bonferroni test.

Supplemental Table 1

Passive and active membrane properties of EGFP+ dorsal horn neurons (3W) classified according to their firing patterns

	Tonic-firing (T; n = 28)	Delayed-firing (D; n = 17)	Phasic-firing (P; n = 6)	Single-Spike (SS; n = 4)	ANOVA (P)
Resting membrane potential (mV)	-61 ± 1	-61 ± 2	-56 ± 3	-64 ± 4	0.13
Input resistance (MΩ)	757 ± 63	811 ± 64	635 ± 64	340 ± 59 * T & D	0.03
Membrane capacitance (pF)	48 ± 3	38 ± 4	53 ± 4	54 ± 4	0.06
Rheobase (pA)	30 ± 2	27 ± 3	55 ± 9	155 ± 50 *** All	< 0.0001
No. of action potentials at rheobase	2.1 ± 0.3	1.9 ± 0.3	1.0 ± 0.0	1.0 ± 0.0	0.21
Delay at rheobase (msec)	217 ± 28	473 ± 65 *** All	94 ± 18	123 ± 63	< 0.0001
CV of interspike intervals (%)	22 ± 3	13 ± 3	69 ± 10 *** T & D	N/A	< 0.0001
Half-width of action potentials (msec)	0.51 ± 0.02	0.45 ± 0.03	0.49 ± 0.06	0.41 ± 0.04	0.12

CV; coefficient of variation

* P < 0.05, *** P < 0.001, one-way ANOVA with post hoc Tukey test